Int. J. Solids Structures Vol. 22, No. 10, pp. 1149–1159, 1986
Printed in Great Britain.

0020–7683/86 $3.00+.00
Pergamon Journals Ltd.

PROPER BACKGROUND CHOICE IN RESONANCE SCATTERING BY ELASTIC SHELLS

G. C. GAUNAURD
Naval Surface Weapons Center, Silver Spring, MD 20903-50000, U.S.A.

and

M. F. WERBY
Naval Ocean R & D Activity, NSTL Station, MS 39529, U.S.A.

(*Received* 8 *March* 1985; *in revised form* 4 *September* 1985)

Abstract—An analytical and computational study of acoustic wave-scattering by submerged spheroidal and spherical shells is presented. The direct scattering calculations displayed here are all accomplished by means of a recently improved *T*-Matrix formulation, suitable for submerged elastic shells, that is faster and more efficient than earlier ones. The study allows the determination of the relative shell-thickness for which the usual *rigid* background of metal objects in water switches to the *soft* one. A key criterion to establish this transitional thickness, and to decide on the proper choice of background, is provided by the relative phase between the elastic form-function of the target and the form-function of either the rigid or the soft background. The relative phase of whichever is the proper background to use to isolate the system's resonances, with respect to the elastic response, will exhibit jumps of π-radians as the system goes through its resonances. The relative phase of the incorrect background with respect to the elastic response will undergo rapid and meaningless oscillations at all frequencies. This behavior serves to reject the incorrect background. The study permits the estimation of the transitional shell-thickness required for the switch in behavior from rigid to soft to occur, which here is $2t/L \approx 10^{-3}$. It is noted that thinner shells will have narrower resonances. Ultimately, very thin shells behave like gas bubbles in liquids. The soft background is found to be the proper choice only for cases where the shell is so thin that they become of little practical value, since they will buckle and collapse under relatively light external pressures. Many results are numerically computed and graphically displayed for plane waves incident on spheroidal elastic shells along their axis of symmetry.

1. INTRODUCTION

The Resonance Scattering Theory (RST) presented and developed for many cases in many papers, and reviewed, by now, in three lengthy book chapters[1–3], has studied the interaction of acoustic, elastic and electromagnetic waves with a variety of targets of various shapes and compositions. The theory has a direct and also an inverse mode of operation. By means of its direct mode, it can predict the scattering behavior of penetrable targets of known shape and composition. If the target characteristics are unknown *a priori*, it is sometimes possible to extract them from the received echo-returns by suitable analysis of the resonance features present in them, via the inverse scattering capability of the technique[3]. The crucial step of the method consists in performing a partial-wave decomposition of the predicted cross-sections, followed by a splitting of each partial-wave or normal-mode into two contributions. The first contribution, called the "background", and totally unrelated to noises present either in the medium or in the sensor system, represents the way in which an otherwise identical scatterer to the one under study, but impenetrable in composition (i.e. not admitting interior fields), would scatter energy within that particular mode. An impenetrable scatterer can be either acoustically soft (i.e. Dirichlet boundary condition) or acoustically rigid (i.e. Neumann boundary condition), which are the two extremes of acoustic impenetrability. If properly chosen, impenetrable, modal backgrounds are subtracted from the modal partial-waves of the original penetrable scatterer, the result is the set of modal resonances of the scatterer. These resonances constitute a unique characteristic of the target and serve to identify it unambiguously. If the shape of the scatterer is complex and/or nonseparable, then the background/resonance decomposition cannot be performed one mode at a time. It can, however, be performed for the summed cross-section, and we will illustrate how this is done for a (nonseparable) spheroidal

shell shape, by means of the T-Matrix Method. The background-subtraction procedure mentioned above can be theoretically achieved by the systematic methodology of the RST[1–3]. The subtraction can also be experimentally accomplished by means of an instrumental implementation that sometimes yields results indistinguishable from the predictions of the RST. This implementation was discovered and originally developed in France by Gerard Maze[4] in 1981, after the appearance of the first few theoretical papers on the RST in 1977–78 which are listed in the reviews[1–3] and elsewhere[5]. The French experimental implementation has reappeared in several articles since 1981, and the most recent one has just appeared in 1984[6]. The work of Maze and Ripoche first dealt with elastic cylinders[4], and later on with hollow tubes[6] and analogous configurations. Recent work in the United States[7, 8] has compared the RST predictions to the experimental observations. Both theory and experiment require the selection of the "proper background", so that the target resonances can be isolated by subtraction. This is achieved theoretically as has been extensively explained before[1–3, 7, 8]. Experimentally, this is achieved by sampling the returned echo-pulse in different portions of its tail-end[4–6]. The precise location within the pulse-tail where the sampling is done, which corresponds to which type of background one ends-up subtracting, is not clearly known *a priori*. Any theoretical, analytical or computational study that can clarify our understanding of the background suppression process, which is indispensable to isolate the true target resonances, will be very helpful in future developments of theory and experimental implementation.

Broad guidelines exist that permit us to gain *a priori* knowledge of the proper background choice. A scatterer that is very tenuous compared to its surroundings will be accurately described by acoustically *soft* backgrounds. A gas bubble in a liquid is an example of this case. Here the impedance mismatch ratio between the two fluids is several thousands to one. If we reverse the fluid roles and we consider a liquid droplet in air, the mismatch ratio is still the same, but in the opposite direction. In this case, the proper background one must subtract in order to isolate the resonances of the scatterer from the cross-section, or its partial-waves, is the *rigid* one. Fluid scatterers within fluid (or solid) media have been well studied for background-subtraction purposes[9] since they are the simplest of penetrable scatterers exhibiting resonances. In these cases where the impedance mismatch ratio is so large, the resonances are always found to be very narrow. For other combinations of substances, such as a water-filled cavity in an aluminum matrix[5], the impedance mismatch ratio is about 6 and the modal resonances can still be isolated via the soft backgrounds, but they turn out to be much wider. The same conclusion holds for a metal sphere in a liquid[10] but now subtracting the acoustically rigid background.

A practical system of great interest is an air-filled elastic shell in water. For realistic three-dimensional applications one should first consider spheroidal and spherical shells. It is only for the spherical shell that an exact solution can be constructed in closed form. It has been shown that no exact general scattering solution is possible for the spheroidal shell, or even for the solid elastic spheroid immersed in a fluid or in a solid[11, 12]. These systems are simply not separable. Only the rigid/soft spheroid in a fluid admits an exact solution[13]. We remark that if the rigid/soft spheroid is embedded in an elastic medium, then the problem becomes nonseparable and only approximate solutions, such as those based on perturbation theory[12], are possible. In view of the analytical difficulties[14] present for the elastic spheroidal body or spheroidal hollow shell in a fluid, we will compute our results for this case by means of a fast extension of the T-Matrix Method[15, 16]. Numerical solutions to these nonseparable problems by computational approaches such as the T-Matrix Method[17] can always be generated. The T-Matrix computational machinery is also used to perform the direct-scattering calculations shown here for spherical shells, even though in this case exact solutions[18] have been developed for situations as general as when they are covered with layers of possibly absorbing materials.

The basic characteristic of the background from any type of shell is that it depends on the shell's thickness (i.e. $(a-b)/a = t/a$) and on its material composition (i.e. its elastic/viscoelastic parameters). It has been pointed out in the past[1, 8, 18] that a metal shell in water has resonances that can be extracted from its sonar cross-section by subtracting the rigid background, unless the shell is very thin, in which case other backgrounds must

be used[18]. In fact, theories for intermediate or transitional backgrounds have already been introduced with success[18]. For very thin shells in water, the "proper" background that isolates the resonances switches from rigid to soft, and the overall scattering behavior of the shell starts to resemble that of a gas bubble[9, 19]. In what follows we will use the improved T-Matrix approach described elsewhere[16, 20], to study the background transition process and the isolation of shell resonances procedure for air-filled spheroidal elastic shells of variable thicknesses and compositions submerged in water. A valid criterion will be given to determine the suitable background choice and the result of its use.

2. SUMMARY OF THE IMPROVED T-MATRIX APPROACH SUITABLE FOR SPHEROIDAL ELASTIC SHELLS IN WATER

We consider elastic shells of any shape under any type of incident acoustic wave, in any direction, but quickly particularize the formulation to backscattering from prolate spheroidal shells when the incidence is along the axis of symmetry (i.e. end-on). Any shell-thickness, material composition and aspect ratio (i.e. the ratio of the spheroid's length L to its widest outer diameter $2a$) is conceivably possible. It is customary to express and display the back-scattered form-function in the far-field, f_∞, as a function of $k_1 L/2$. The shell's sonar cross-section is proportional to $|f_\infty|^2$. The outer fluid is medium 1, the shell itself is medium 2 and the interior gas is medium 3. The boundary conditions at the two solid/fluid interfaces are statements of continuity of stresses and displacements and they have the form

$$\hat{n}\cdot\mathbf{u}_+ = \hat{n}\cdot\mathbf{u}_-, \qquad \hat{n}\cdot\mathbf{t}_+ = \hat{n}\cdot\mathbf{t}_-, \qquad \hat{n}\times\mathbf{t}_+ = \hat{n}\times\mathbf{t}_-. \tag{1}$$

Here $\hat{n}$ is the outward normal to the shell, $\mathbf{u}$ is the displacement field and $\mathbf{t}$ is the traction vector, which is related to the displacements by the relation

$$\mathbf{t} = \hat{n}\cdot[\lambda\vec{\mathbf{I}}\nabla\cdot\mathbf{u}+\mu(\nabla\mathbf{u}+\mathbf{u}\nabla)]. \tag{2}$$

Following standard nomenclature[15–17, 22] we can construct the exterior and interior integral representation for the fields in the various regions. After matching these solutions at the boundaries one can construct a unique[21] solution to the (direct) scattering problem.

The T-Matrix Method relates incident to scattered fields, with the scattered field subject to the boundary conditions present at the scatterer, and to the Sommerfeld boundary condition at infinity. The incident and scattered fields, ψ^i and ψ^s, are defined

$$\psi^i \equiv \sum_j A_j \,\mathrm{Re}\,\psi_j, \qquad \psi^s \equiv \sum_j F_j\psi_j, \tag{3}$$

where A_j, F_j are the partial-wave coefficients of the incident and scattered fields and where ψ_j designates some appropriate basis vector state. The T-Matrix Method merely relates these coefficients in the form

$$F_i = \sum_j T_{ij} A_j, \tag{4}$$

where the T_{ij} are the T-Matrix elements. Using the exterior and the interior (Helmholtz) boundary integral equations for the fields at the various regions, together with an expansion procedure in partial waves using appropriate basis vector sets, the final expression for the T-Matrix turns out to be

$$T = -[(Q_{RR}-Q_{RO}T_2)(R_R+R_OT_2+iT_2)^{-1}P][(Q_{OR}-Q_{OO}T_2)(R_R+R_OT_2+iT_2)^{-1}P]^{-1}, \tag{5}$$

where the various matrixes Q, R, P and T_2 are defined by the following expressions:

$$Q_{\binom{OO}{RR}^{ij}} = \frac{k_1^3}{\rho_1\omega^2}\iint_S \left\{\lambda_1 \nabla\cdot\left[\binom{Ou}{Re}\psi_n^{(1)}\right]\left[\hat{n}\cdot\binom{Ou}{Re}\psi_{ij}^{(2)}\right] - \left[\hat{n}\cdot\binom{Ou}{Re}\psi_n^{(1)}\right]\hat{n}\cdot\mathbf{t}_2\binom{Ou}{Re}\psi_{ij}^{(2)}\right\} dS,$$

$$R_{\binom{O}{R}^{ij}} = \frac{k_{s_2}^3}{\rho_2\omega^2}\iint_S \left\{\mathbf{t}_2\left[\binom{Ou}{Re}\psi_{ij}^{(2)}\right]\cdot\left[\binom{Ou}{Re}\psi_{ij}^{(2)}\times n\right] - \left[\hat{n}\cdot\binom{Ou}{Re}\psi_{ij}^{(2)}\right](\hat{n}\cdot\mathbf{t}_2)\left[\binom{Ou}{Re}\psi_{ij}^{(2)}\right]\right\} dS,$$

$$P_{ij} = \frac{k_{s_2}^3}{\rho_2\omega^2}\iint_S [\hat{n}\cdot\mathbf{t}_2(Re\,\psi_{ij}^{(2)})\hat{n}\cdot\psi_n^{(1)}]\cdot dS, \qquad T_2 = -Re\,Q_2(Q_2)^{-1}. \tag{6}$$

It is clear that $\psi_n^{(1)}$ and $\psi_{ij}^{(2)}$ describe the basis vectors in the fluid and solid, respectively, and that T_2 refers to scattering from the inner shell surface. The above final form of the T-Matrix Method has some numerical deficiencies. An improved expression was introduced[15] to simplify some of the complications, and to reduce the required number of expansion terms. The improved expression is

$$T = (\hat{u}\hat{G}^* - I)/2, \tag{7}$$

where

$$\begin{aligned} \hat{G} &= [(Q_{OR} + Q_{OO}T_2)M^{-1}P], \\ \hat{u} &= [(Q_{RR} + Q_{RO}T_2)M^{-1}P - 2G], \\ M &= R_R + R_O T_2 + iT_2. \end{aligned} \tag{8}$$

In this form, the method includes the generalized optical theorem (energy conservation) and symmetry properties as constraints and, thus, it has the added advantage of yielding symmetric solutions satisfying energy conservation conditions, as is required of non-lossy scatterers. The spheroidal shell calculations presented in this paper make use of this latter form of the T-Matrix Method. The method generates the form-function f_∞ by the formula

$$f_\infty(\theta, k_1 L/2) = \left|\frac{2}{kL/2}\sum_{n=0}^{\infty}\sum_{m=0}^{\infty}(-1)^{n+1}P_n(\cos\theta)\varepsilon_{nm}T_{nm}A_m\right|, \tag{9}$$

where P_n are the usual Legendre polynomials, and ε_{nm} are normalization constants given by

$$\varepsilon_{nm} = \sqrt{\left(\frac{(2n+1)\,(n-m)!}{4\pi(n+m)!}\varepsilon_m\right)}, \tag{10}$$

where $\varepsilon_m = 2 - \delta_{m0}$. In the back-scattering direction $\theta = \pi$ the above expression reduces further in view of the relation $P_n(\cos\pi) = (-1)^n$. We repeat that for spheroidal solid bodies or spheroidal shells, the exact scattering problem cannot be solved by means of series [11, 14] since it is not possible to satisfy all boundary conditions on the surface(s) of the scatterer. Only approximate numerical solutions are possible for these cases. We are not aware of any prior numerical solution for *shells*.

3. RESONANCE SCATTERING FOR SPHERICAL ELASTIC SHELLS

The case of the spherical shell can be obtained from the above T-Matrix formulation where the aspect ratio $L/2a$ becomes unity. In this case, however, an exact, separable solution is possible in closed-form, and this has been obtained before[18], even when the shell is layered. The basic point of the RST can be illustrated very clearly in this case because

the scattering amplitude of its nth partial-wave can be exactly expressed by the relation

$$|f_n(\pi)| = \left| \frac{2n+1}{k_1 a} e^{2i\xi_n^{(r)}} \left(\frac{z_2^{-1} - z_1^{-1}}{\text{Re } z_1^{-1} - F_n^{-1} + i \text{ Im } z_1^{-1}} + 2i \, e^{-i\xi_n^{(r)}} \sin \xi_n^{(r)} \right) \right| \tag{11}$$

which shows the two interacting terms corresponding to shell resonances due to the shell's penetrability (i.e. first term within the bracket), and smooth modal backgrounds due to the shell's shape, assumed impenetrable (i.e. second term). Such analytic expression, so clearly showing the interaction of these two contributions, cannot be given for a spheroidal shell, although their effect on the summed form-function can be *numerically* computed. The denominator of the first term, whose vanishing indicates the presence of a shell resonance, can be written in polar form

$$d = \rho_n \exp(i\alpha_n), \tag{12}$$

where

$$\rho_n = [(\text{Re } z_1^{-1} - F_n^{-1})^2 + (\text{Im } z_1^{-1})^2]^{1/2}, \tag{13}$$

$$\alpha_n = \arctan [\text{Im } z_1^{-1} / (\text{Re } z_1^{-1} - F_n^{-1})], \tag{14}$$

and where all the quantities z_1, z_2, F_n and $\xi_n^{(r)}$ were given earlier[18]. It is evident that the roots of the characteristic equation: $\text{Re } z_1^{-1} = F_n^{-1}$ are the real resonances of the fluid-loaded shell. Clearly α_n is the relative phase of the resonances, given in the first term within the bracket in eqn (11), with respect to the (rigid) backgrounds in the second term. Every time the system goes through a resonance, the characteristic equation is identically satisfied, and in view of eqn (14), the relative phase α_n goes through a jump of π-radians. We have displayed these phase jumps earlier[5b] in simpler configurations. The analysis of the relative phase α_n is a very crucial criterion to determine whether the background being used properly describes the passage of the system through its resonances. Such criterion can be used to accept or reject a background as the proper isolator of the system's resonances. Although for a spheroidal shell an exact expression such as that in eqn (11) cannot be produced, one can always numerically compute the relative phase α_n and examine it for jumps of π-radians as in the spherical case. If they are present, one can conclude that the proper choice of background was made to compute it, and there lies the usefulness of this parameter for a shell of arbitrary shape.

4. NUMERICAL RESULTS AND DISCUSSION

We will consider aluminum and steel shells, air-filled, and immersed in water. The properties of these substances are summarized in Table 1.

After numerous calculations we can conclude that for most metal shells in water, the background that once subtracted isolates the resonances, is the *rigid* one. This statement holds until the shell becomes very thin. Figure 1 illustrates the situation that is observed for shells down to 1% in relative thickness. The top graph on Fig. 1 is the complete elastic

Table 1. ($i = 1, 2$ or 3)

	Property		
Medium	ρ_i (g/cm^3)	c_i or c_{d_i} (cm/s)	c_{s_i} (cm/s)
1. Water	1.0	1.4825×10^5	—
2. Aluminum	2.7	6.42×10^5	3.04×10^5
2. Steel	7.7	5.95×10^5	3.24×10^5
3. Air	0.012	0.344×10^5	—

response plotted in the band $3.0 \leqslant k_1 L/2 \leqslant 15.0$, from eqn (9), for an air-filled prolate spheroidal aluminum shell in water. The incidence is end-on, along the symmetry axis. The aspect ratio (i.e. length-to-diameter) of the spheroid is $L/2a = 1.75$, which is close to the upper limit that can be computed with present day T-Matrix algorithms, as described here. The second graph in Fig. 1 shows the result of subtracting the *rigid* background. Resonance

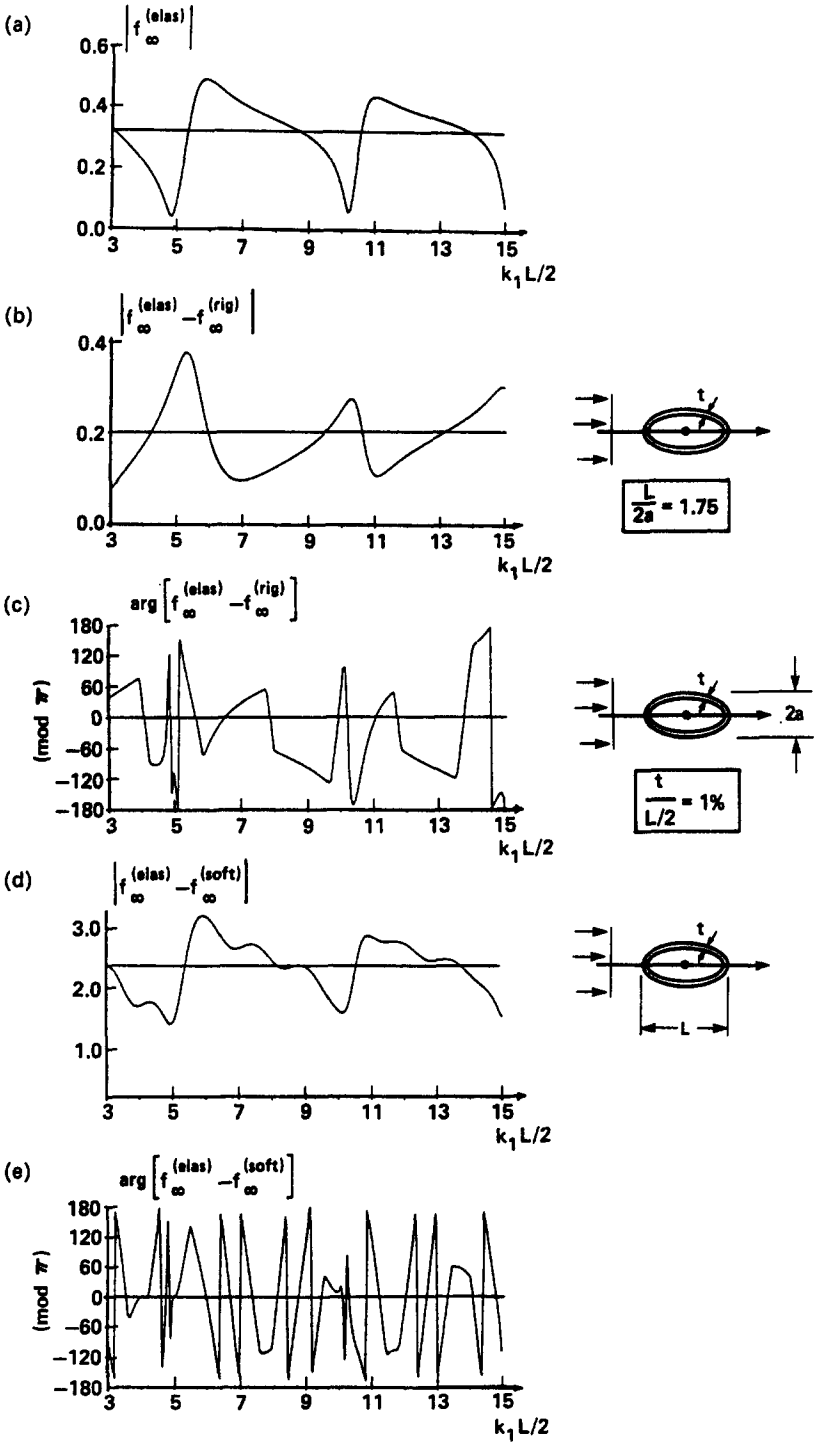

Fig. 1. Scattering of a plane acoustic wave by a spheroidal aluminum shell at end-on (bow) incidence. The spheroidal shell has aspect ratio $L/2a = 1.75$ and relative thickness $2t/L = 1\%$. (a) Elastic response vs $k_1 L/2$. (b) Subtraction of the *rigid* background isolating the system's resonances. (c) The phase of $f^{elas} - f^{rig}$ in (b), showing the π-radian jumps. (d) Subtraction of the soft background. (e) Phase of the difference $f^{elas} - f^{soft}$, showing rapid, unexplainable oscillations. [From eqns (5)–(9).]

peaks are clearly isolated. The third graph shows the phase (mod π) of the difference displayed in the second graph exhibiting the jumps of π-radians at the locations of the resonances. The fourth graph displays the result of subtracting the *soft* backgrounds. This graph shows no clear resonance-type peak. The fifth graph shows the phase of the difference between the elastic response in the top graph and that of the soft background. This phase jumps wildly at all frequencies and does not exhibit the expected behavior of the "proper" background, and therefore serves to reject the *soft* background in this case.

Below 1% relative-thickness things begin to change, and when we have reached $2t/L = 0.1\%$, for the same aspect ratio $L/2a = 1.75$ and materials, it is the *soft* background that isolates the resonances. Figure 2 illustrates the situation. The top graph is the summed elastic response, as found from eqn (9). The second graph shows the result of subtracting the *soft* background. It is now the subtraction of the *soft* background that isolates the resonance peaks, which are quite evident. The third graph shows the phase of the difference $f^{(\text{elas})} - f^{(\text{soft})}$, which shows the jumps of π-radians at the system's resonances. The *rigid* background is subtracted from the elastic response in the fourth graph, which does not show any resonance peak or behavior. The phase of this difference, shown in the fourth graph, is now displayed on the fifth graph. The erratic oscillations of this phase demonstrate the unsuitability of the *rigid* background and serve to reject it in this case.

The thinner the shell-thickness, the clearer it becomes that it is the *soft* background that isolates the system's resonances. Figure 3 clearly demonstrates this point. This figure is calculated for an air-filled spherical *steel* shell in water of relative thickness $t/a = 0.01\%$, in the spectral band $2.0 \leqslant k_1 a \leqslant 11.0$. The shell is now very thin and, although its material composition is stiffer, it is so thin that it is behaving much like a bubble[9, 19]. The calculations shown in Fig. 3 were done using the T-Matrix (numerical) formulation given in eqn (9), and also by means of the exact formulation[18] described in Section 3. The top graph shows the elastic response. The second graph displays the modulus of the difference between the elastic response and the *soft* background. Resonance peaks are not only clearly isolated but they are visibly narrower than in Fig. 2. This is due to the fact that the shell is now thinner and behaving like a bubble[9, 19]. The third graph shows the phase of the difference shown in the second graph, which clearly exhibits the expected phase-jumps at the locations of the resonance frequencies. Subtraction of the *rigid* background is displayed in the fourth graph, which does not exhibit any resonance behavior. The phase of this unsuitable difference $f^{(\text{elast})} - f^{(\text{rig})}$ is shown in the fifth graph. Its rapid, unexplainable oscillations at all frequencies serve to reject the *rigid* background as the proper resonance isolator, just as in Fig. 2 (fifth graph).

Intermediate plots, not shown here, show that for an aluminum shell in water, the relative thickness for which the proper background switches from rigid to soft, is about $2t/L \approx 0.1\%$ as shown in Fig. 2. The resonances, isolated in the second graphs of Figs. 1, 2 and 3, are progressively narrower in these figures as the shell becomes thinner. Sound penetration into this elastic structure takes place through the spectral windows centered around each one of the system's resonances isolated in these second graphs. The RST literature has made this point many times before[1–3], for simpler, separable configurations.

5. ELASTIC STABILITY CONSIDERATIONS

Spherical shells are the most stable of all shells. The external actual pressure that would trigger the buckling of a spherical shell is about one-third of the ideal buckling pressure. This ideal pressure is known to be[23]

$$p' = \frac{2Et^2}{a^2\sqrt{3(1-\nu^2)}}, \tag{15}$$

which for steel (i.e. $E = 3 \times 10^7$ psi and $\nu = 0.3$) and a relative thickness of $t/a = 10^{-3} = 0.1\%$, comes out to be $p' = 36$ psi. The actual buckling pressure is about 12 psi. For spheroidal shells the actual buckling pressure is smaller than that for spherical

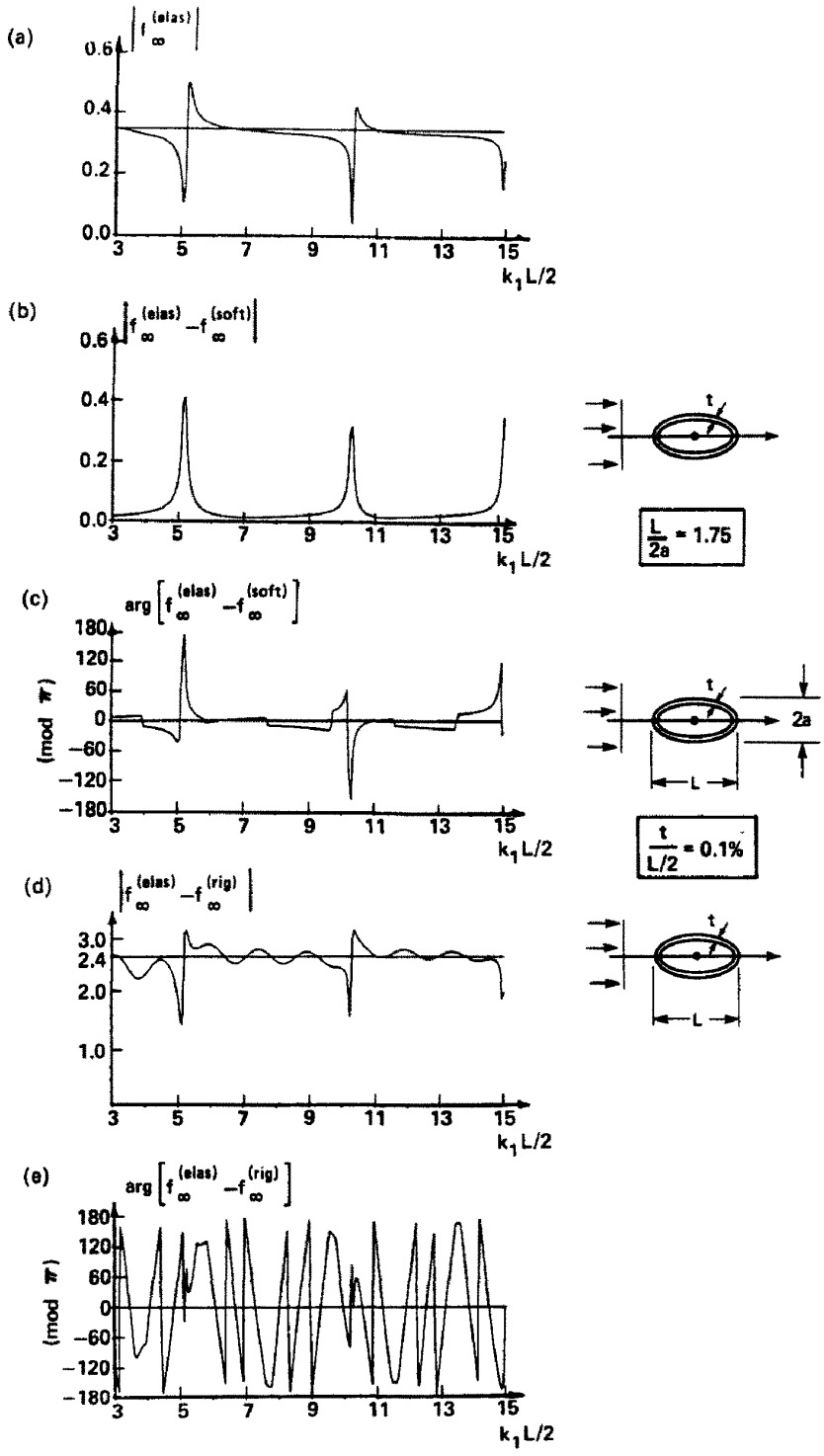

Fig. 2. Same as in Fig. 1 but for a spheroidal aluminum shell of thickness $2t/L = 0.1\%$. (a) Elastic response vs $k_1 L/2$. (b) Subtraction of the *soft* background, which isolates the system's resonances. (c) The phase of the difference in (b) showing the π-radian jumps. (d) Subtraction of the rigid background. (e) Phase of the difference displayed in (d), showing rapid, meaningless oscillations at all frequencies.

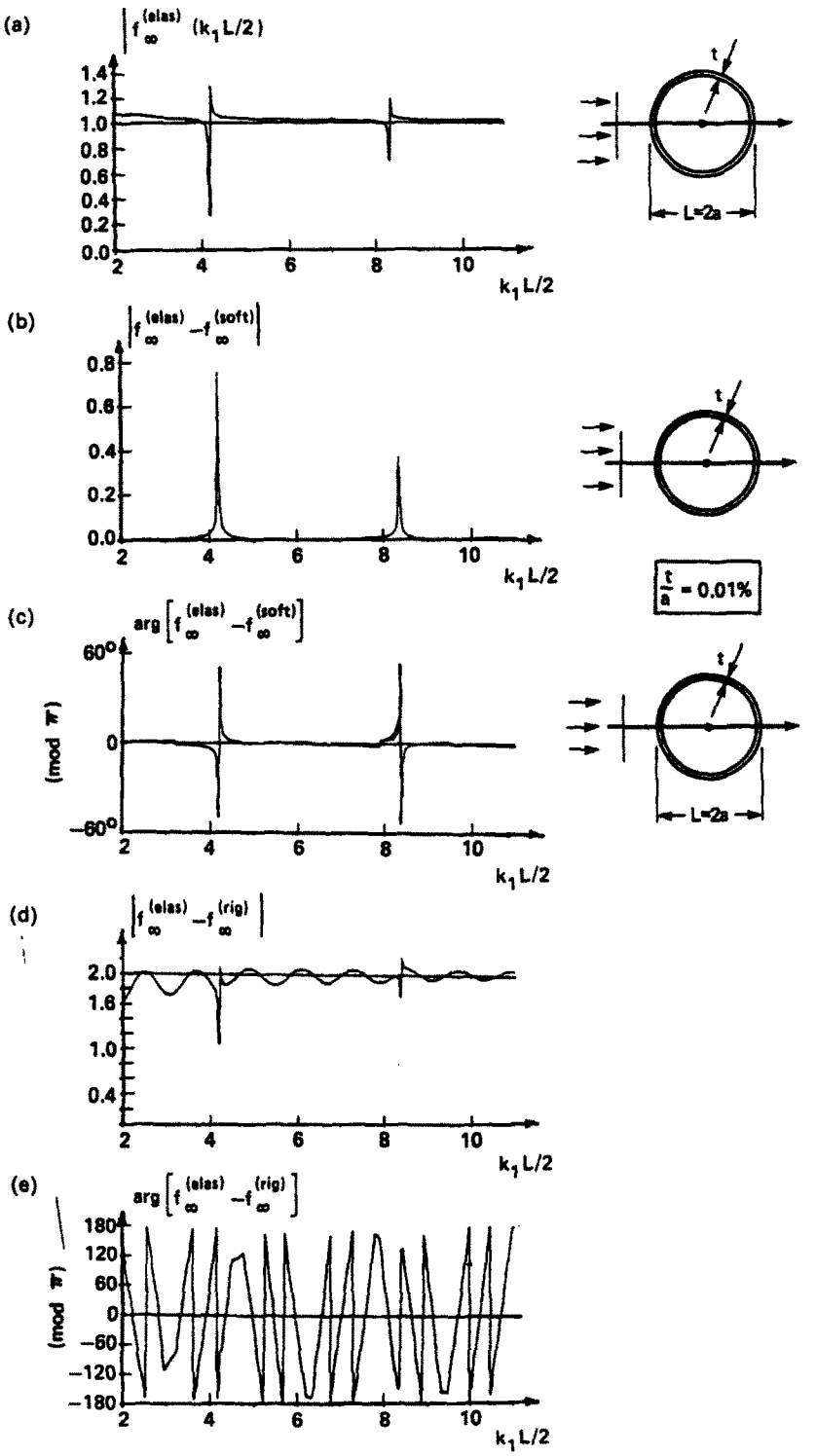

Fig. 3. Scattering of a plane sound wave by a spherical steel shell in water of thickness $t/a = 0.01\%$. (a) Elastic response vs k_1a. (b) Subtraction of the *soft* background which isolates the resonances. (c) The phase of the difference in (b) showing the π-jumps. (d) Subtraction of the (incorrect) rigid background. (e) Phase of the difference shown in (d), exhibiting rapid and unexplainable oscillations at all frequencies that serve to reject the rigid background in this case.

shells, and it becomes even smaller for larger aspect ratios. This means that shells for which the soft background is the one that isolates the resonances must be so thin (i.e. $2t/L < 0.1\%$, for aluminum and aspect ratio: $L/2a = 1.75$) that they buckle very easily. Thus, such extremely thin shells become unacceptable from the point of view of their elastic stability, since they would buckle within a few feet of the water surface.

6. CONCLUSIONS

The present paper shows an analytical and computational study of sound scattering from thin, air-filled, elastic, spheroidal and spherical shells in water that allows us to determine the transitional shell-thickness for which the usual rigid background of metal objects in water switches to the soft one. A key criterion to establish this transition thickness and to decide on the proper choice of background, is provided by the phase of the differences $[f_\infty^{elas} - f_\infty^{rig}]$ and $[f_\infty^{elas} - f_\infty^{soft}]$ between the elastic response and either the rigid or soft backgrounds. The relative phase of whichever is the proper background to accomplish the isolation (and display) of the shell resonances from the back-scattered return, will exhibit jumps of π-radians, as the frequency is increased and the system goes through its resonances. The phase of whichever is the incorrect background relative to that of the elastic (form-function) response, will perform rapid and wild oscillations in a meaningless or unexplainable fashion for all frequencies in the pertinent band. The calculations displayed here are all performed by means of an improved T-Matrix approach[16] suitable for submerged spheroidal shells. The case of the spherical shell (Fig. 3) was also done by means of the exact solution, which is available[18], as a check. All the calculations show that t/a (or $2t/L$) of about 10^{-3} is the transition thickness below which the background becomes *soft*. The thinner the shells are, the narrower its resonances will become, and their behavior will resemble that of bubbles in liquids[5, 9, 19]. This bubble-like behavior for $2t/L \leqslant 0.1\%$, although quite real, is of questionable usefulness, because we have shown that such thin shells will buckle easily under relatively small (i.e. below 12 psi) external pressures. The present study was carried on to show that direct-scattering numerical predictions are possible for spheroidal shells in wide frequency bands, via the improved T-Matrix formulation presented here. The study also proves the existence of the scattering behavior of spheroidal shells requiring the use of the *soft* background to isolate its resonances. It also permits the estimation of the value of the transitional shell-thickness required for this unexpected switch in behavior to occur. The relative phase between the elastic response and the "proper" background emerges as the key criterion to select the correct background that isolates the resonances of the shell, whatever its shape. We have computed and graphically displayed many actual shell-resonances from the echoes that are accurate in spectral location and in shape (i.e. width and amplitude). The entire procedure assumes that the shell motions are described by the exact 3-dimensional equations of elasticity, no approximate shell-theory having been introduced. Portions of this work were presented at a professional society meeting[24].

Acknowledgement—The authors wish to thank the Independent Research Board of the Naval Surface Weapons Center and the Naval Ocean Research and Development Activity, as well as the Naval Electronics Systems Command (ELEX-612) and the Office of Naval Research for support and encouragement.

REFERENCES

1. G. Gaunaurd and H. Uberall, Resonances in acoustic and in elastic wave-scattering. In *Recent Developments in Classical Wave Scattering* (Edited by V. K. Varadan and V. Varadan), pp. 413–430. Pergamon Press, New York (1980).
2. L. Flax, G. Gaunaurd and H. Uberall, The theory of resonance scattering. In *Physical Acoustics XV* (Edited by W. P. Mason and R. N. Thurston), Chap. 3, pp. 191–294. Academic Press, New York (1981).
3. G. Gaunaurd, H. Uberall and L. Dragonette, Inverse scattering and the resonances of viscoelastic and electromagnetic systems. In *Wave Propagation in Viscoelastic Media* (Edited by F. Mainardi), pp. 234–257. Pitman, London (1982).
4. G. Maze, B. Taconet and J. Ripoche, Influence of the whispering gallery waves on the scattering of a plane ultrasonic wave by a cylinder. *Phys. Lett. A* **84**, 309–312 (1981). (In French.)

5. G. Gaunaurd (a) Resonance theory of elastic and viscoelastic wave-scattering and its applications to the spherical cavity in absorptive media. In *Modern Problems in Elastic Wave Propagation* (Edited by J. Miklowitz and J. Achenbach), p. 550. Wiley, New York (1977). (b) *J. Acoust. Soc. Am.* **63**, 1699–1712 (1978).
6. G. Maze, J. Ripoche *et al.*, Resonance response of elastic cylinders. *Rev. CETHEDEC, Ondes Signal* **78**, 73–93 (1984). (In French.)
7. D. Brill and G. Gaunaurd, Acoustic resonance scattering by a penetrable cylinder. *J. Acoust. Soc. Am.* **73**, 1448–1455 (1983).
8. G. Gaunaurd and D. Brill, Acoustic spectrogram and complex-frequency poles of a resonantly excited elastic tube. *J. Acoust. Soc. Am.* **75**, 1680–1693 (1984).
9. G. Gaunaurd, Multipole resonances... in acoustic wave—scattering from bubbles and droplets, In *Mathematical Methods and Applications of Scattering Theory* (Edited by A. W. Saenz), pp. 114–120. Springer, Berlin (1979).
10. G. Gaunaurd and H. Uberall, RST analysis of monostatic and bistatic acoustic echoes from an elastic sphere. *J. Acoust. Soc. Am.* **73**, 1–12 (1983).
11. Y. H. Pao, Elastic waves in solids. *J. Appl. Mech.* **50**, 1152–1164 (1983).
12. M. A. Oien and Y. H. Pao, Scattering of compressional waves by a rigid spheroidal inclusion. *J. Appl. Mech. E40*, 1073–1077 (1973).
13. J. J. Bowman *et al.* (Editors), *Electromagnetic and Acoustic Scattering by Simple Shapes*. North-Holland, Amsterdam (1969).
14. A. Silbiger, Scattering of sound by an elastic prolate spheroid. *J. Acoust. Soc. Am.* **35**, 564–570 (1963).
15. M. F. Werby and L. Green, An extended unitary approach for acoustical scattering from elastic shells immersed in fluids. *J. Acoust. Soc. Am.* **74**, 625–630 (1983).
16. M. F. Werby, A coupled higher-order *T*-matrix. *J. Acoust. Soc. Am.* (1986), in press.
17. P. Waterman, Matrix theory of elastic wave-scattering. *J. Acoust. Soc. Am.* **60**, 567–580 (1976).
18. G. Gaunaurd and A. Kalnins, Resonances in the sonar cross-sections of layered spherical shells. *Int. J. Solids Structures* **18**, 1083–1102 (1982).
19. G. Gaunaurd *et al.*, Giant monopole resonances in the scattering of sound waves from air-filled spherical cavities and bubbles. *J. Acoust. Soc. Am.* **64**, 573–594 (1979).
20. M. F. Werby, Numerical treatment of scattering from submerged objects. *J. Acoust. Soc. Am.* **76**, S68 (Invited paper, FF4) (1984).
21. This is to be contrasted to the Helmholtz Integral Equation Method (HIEM) which fails at the internal eigenfrequencies.
22. A. Bostrom, Scattering of stationary acoustic waves by an elastic obstacle immersed in a fluid. *J. Acoust. Soc. Am.* **67**, 390–398 (1980); **67**, 1904–1913 (1980).
23. R. J. Roark, *Formulas for Stress and Strain*, 4th edn, Table XVI (T), p.354. McGraw-Hill, New York (1965).
24. G. C. Gaunaurd and M. F. Werby, Criteria for suitable background choices in resonance acoustic scattering by shells. *J. Acoust. Soc. Am.* **76**, S8 (Paper D-9) (1984).